

Scaling up ecosystem productivity from patch to landscape: a case study of Changbai Mountain Nature Reserve, China

Na Zhang · Zhenliang Yu · Guirui Yu ·
Jianguo Wu

Received: 16 July 2005 / Accepted: 5 July 2006 / Published online: 5 August 2006
© Springer Science+Business Media B.V. 2006

Abstract Scaling up ecosystem processes from plots to landscapes is essential for understanding landscape structure and functioning as well as for assessing ecological impacts of land use and climate change. This study illustrates an upscaling approach to studying the spatiotemporal pattern of ecosystem processes in the Changbai Mountain Nature Reserve in northeastern China by integrating simulation modeling, GIS, remote sensing data, and field-based observations. The ecosystem model incorporated processes of energy transfer,

plant physiology, carbon dynamics, and water cycling. Using a direct extrapolation scheme, the patch-level ecosystem model was scaled up to quantify the landscape-level pattern of primary productivity and the carbon source-sink relationship. The simulated net primary productivity (NPP) for the entire landscape, consisting of several ecosystem types, was $0.680 \text{ kg C m}^{-2} \text{ yr}^{-1}$. The most widely distributed ecosystem type in this region was the mixed broad-leaved and Korean pine (*Pinus koraiensis*) forest, which had the highest NPP ($1.084 \text{ kg C m}^{-2} \text{ yr}^{-1}$). The total annual NPP for all ecosystem types combined was estimated to be $1.332 \text{ Mt C yr}^{-1}$. These results suggest that the Changbai Mountain landscape as a whole was a carbon sink, with a net carbon sequestration rate of about $0.884 \text{ Mt C yr}^{-1}$ for the study period. The simulated NPP agreed reasonably well with available field measurements at a number of locations within the study landscape. Our study provides new insight into the relationship between landscape pattern and ecosystem processes, and useful information for improving management practices in the Changbai Mountain Nature Reserve, which is one of the most important forested landscapes in China. Several research needs are discussed to further refine the modeling approach and reduce prediction uncertainties.

N. Zhang (✉)
College of Resources and Environment, Graduate
University of Chinese Academy of Sciences, 19A Yu
Quan Road, 3908, Beijing 100049, P.R. China
e-mail: zhangna@gucas.ac.cn

Z. Yu
National Natural Science Foundation of China,
Beijing 100085, China

G. Yu
Institute of Geographic Sciences and Natural
Resources Research, Chinese Academy of Sciences,
Beijing 100101, China

J. Wu
School of Life Sciences, Beijing Normal University,
Beijing 100875, China

J. Wu
School of Life Sciences and Global Institute of
Sustainability, Arizona State University, Tempe, AZ
85287, USA

Keywords Scaling · Extrapolation · Ecosystem modeling · Biogeochemical cycles · Landscape

pattern · Net primary productivity · Changbai Mountain Nature Reserve

Introduction

Understanding effects of landscape heterogeneity on ecosystem processes is a key research topic in landscape ecology (Turner et al. 2001; Wu and Hobbs 2002; Turner and Cardille 2006). Because of difficulties in conducting field experiments with ecosystem processes on broader scales, spatially explicit models have become an indispensable tool for addressing this important research topic (Wu et al. 2006). Such models must consider both landscape heterogeneity and ecosystem processes simultaneously on a range of scales. While ecosystem process models have been well developed at the patch or stand level (e.g., Parton et al. 1987; Running and Coughlan 1988; Waring and Running 1998), the emphasis has been on ecophysiological and biogeochemical mechanisms with little consideration of the impacts of spatial heterogeneity. On the other hand, most existing landscape models are sophisticated in treating spatial heterogeneity, but tend to have little detail in biogeochemistry. Mechanistic details in these models focus mostly on demography and disturbances (e.g., Wu and Levin 1994, 1997; Mladenoff and Baker 1999). Since the 1990s, there has been an increasing emphasis on integrating ecosystem processes with landscape pattern (Burke et al. 1990; Band et al. 1991; Coughlan and Running 1997; Aber et al. 1999; Hong et al. 2006; Kennedy et al. 2006). Nevertheless, more studies with different types of ecosystems are needed to improve our understanding of the spatial heterogeneity and scaling relations of ecosystem processes (Wu and Hobbs 2002; Turner and Cardille 2006).

In particular, modeling net primary productivity (NPP) of terrestrial ecosystems is critically important for quantifying carbon sinks and sources on regional and global scales and assessing the consequences of land use and global climate change. While China has a diversity of globally important ecosystems, research in spatial modeling of biogeochemical cycling is still lacking. To address this problem in particular and to improve our understanding of spatial dynamics of ecosys-

tem processes in heterogeneous landscapes in general, we have developed a multi-scaled forest landscape productivity model (FLPM) for one of the most productive reforested areas in northeastern China, the Changbai Mountain Nature Reserve (CMNR). The primary goal of this study was to quantify the spatial pattern of ecosystem productivity and assess the carbon source-sink relationship at the landscape level. In this paper, we will describe the model, present simulation results, examine the results in relation to environmental factors, and discuss the findings and future research directions.

Study site

CMNR is located in northeastern China (127° 42'55"–128° 16'48"E and 41° 41'49"–42° 25'18"N), with an area of 190,582 ha. The reserve, established in 1960, has been a key member of the Chinese Ecosystem Research Network administered by the Chinese Academy of Sciences. CMNR has several types of ecosystems along the elevation gradient (Fig. 1): the mixed broad-leaved and Korean pine (*Pinus koraiensis*) forest (720–1,100 m), the spruce-fir (*Picea jezoensis*, *Picea koraiensis*, *Abies nephrolepis*) forest (1,100–1,800 m), the sub-alpine *Betula ermanii* forest (1,800–2,100 m), and alpine tundra (above 2,100 m). In addition, there exist several localized plant communities, including Changbai larch (*Larix olgensis*) dominated forests in lowland areas, poplar and birch (*Populus davidiana*, *Betula platyphylla*) forests, ravine meadows, shrubs, and alpine barren lands (Xing 1988). This diversity of vegetation types generally corresponds to the spatial heterogeneity of meteorological conditions in this region (Fig. 2). Among all the vegetation types, the mixed broad-leaved and Korean pine forest and the spruce-fir forest are the most extensive in area (Table 1).

Model description

The model, FLPM, was developed based on boreal ecosystem productivity simulator (BEPS) (Liu et al. 1997, 1999), with reference to Forest-

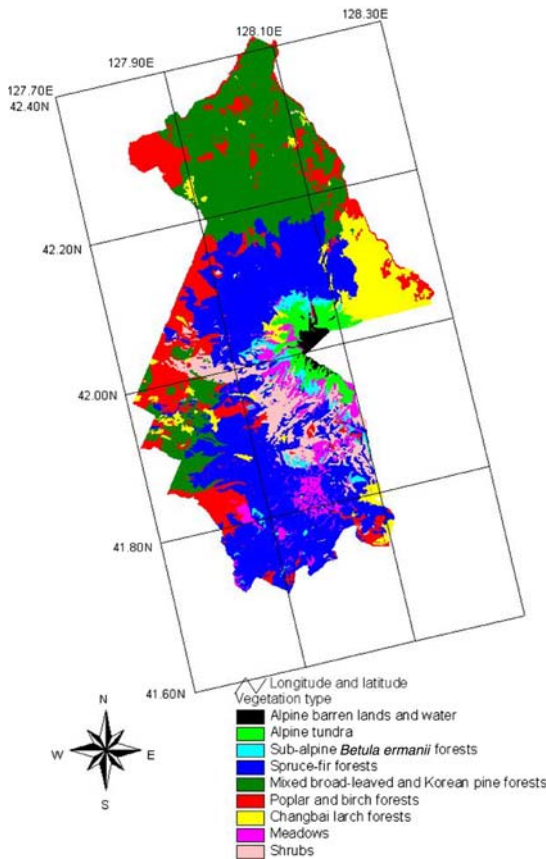


Fig. 1 Vegetation map of the Changbai Mountain Nature Reserve in 1995

BGC (Running and Coughlan 1988) and BIOME-BGC (Running and Hunt 1993). One of the major improvements in BEPS was the implementation of a modified daily canopy photosynthesis module with an innovative temporal and spatial scaling scheme (Chen et al. 1999; Sun et al. 2004). FLPM consists of four submodels: (1) the energy transfer submodel, (2) the physiological regulation submodel, (3) the water cycle submodel, and (4) the carbon cycle submodel. Here we only briefly describe these submodels because more details can be found elsewhere (Liu et al. 1997, 1999; Chen et al. 1999; Zhang et al. 2003d).

The energy transfer submodel computes leaf irradiance and leaf area index (LAI). Based on Norman (1982) and Chen et al. (1999):

$$S_{\text{sun}} = S_{\text{dir}} \times \cos\alpha / \cos\theta + S_{\text{shade}} \quad (1)$$

where S_{sun} is the sunlit leaf irradiance (W m^{-2}), S_{dir} is the direct radiation over the plant canopy

(W m^{-2}), S_{shade} is the radiation over shaded leaves (W m^{-2}), α is the mean distribution angle of sunlit leaves (set as 60°), and θ is the solar zenith angle. The fraction of sunlit leaves (f_{sun}) is modeled as an exponential decay function from the canopy top downward, and the fraction of shaded leaves is simply: $f_{\text{shade}} = 1 - f_{\text{sun}}$. Sunlit LAI (LAI_{sun}) is the integral of f_{sun} (Dai et al. 2004):

$$\begin{aligned} \text{LAI}_{\text{sun}} &= \int_0^{\text{LAI}} f_{\text{sun}}(x) dx = \int_0^{\text{LAI}} e^{-k_b x} dx \\ &= \frac{1}{k_b} (1 - e^{-k_b \text{LAI}}) \end{aligned} \quad (2)$$

where x is the cumulative LAI measured downwards from the canopy top, and k_b is the direct beam extinction coefficient of the canopy.

The physiological regulation submodel simulates stomatal conductance (g_s) and total conductance for sunlit and shaded leaves as follows:

$$\begin{aligned} g_s &= \max[g_{s,\text{max}} \times f(\text{PPFD}_n) \times f(T) \times f(\text{VPD}) \\ &\times f(\text{LWP}) \times f(\text{CO}_2) \times f(T_m) \times g_{\text{corr}} \cdot g_{s,\text{min}}] \end{aligned} \quad (3)$$

where $g_{s,\text{max}}$ and $g_{s,\text{min}}$ are the species-dependent maximum and minimum conductance, PPFD_n is the photosynthetic photon flux density at noon ($\mu \text{mol m}^{-2} \text{s}^{-1}$), T is the mean daytime air temperature ($^\circ\text{C}$), VPD is the vapor pressure deficit (kPa), LWP is the leaf water potential (MPa), CO_2 is the intercellular CO_2 concentration, and T_m is the freezing night minimum temperature ($^\circ\text{C}$), and g_{corr} is a correlation factor of g_s with temperature and pressure. The canopy conductance (G_s) is computed based on LAI of sunlit and shaded leaves:

$$G_s = g_{\text{sp}} \times \text{LAI}_{\text{sun}} + g_{\text{sn}} \times \text{LAI}_{\text{shade}} \quad (4)$$

where g_{sp} and g_{sn} are the stomatal conductance for sunlit and shaded leaves, respectively.

The water cycle submodel simulates soil water dynamics determined by precipitation and snowmelt as well as soil evaporation, canopy interception evaporation, understory and litter layer interception evaporation, canopy transpiration, and surface runoff. In this study, soil water loss to

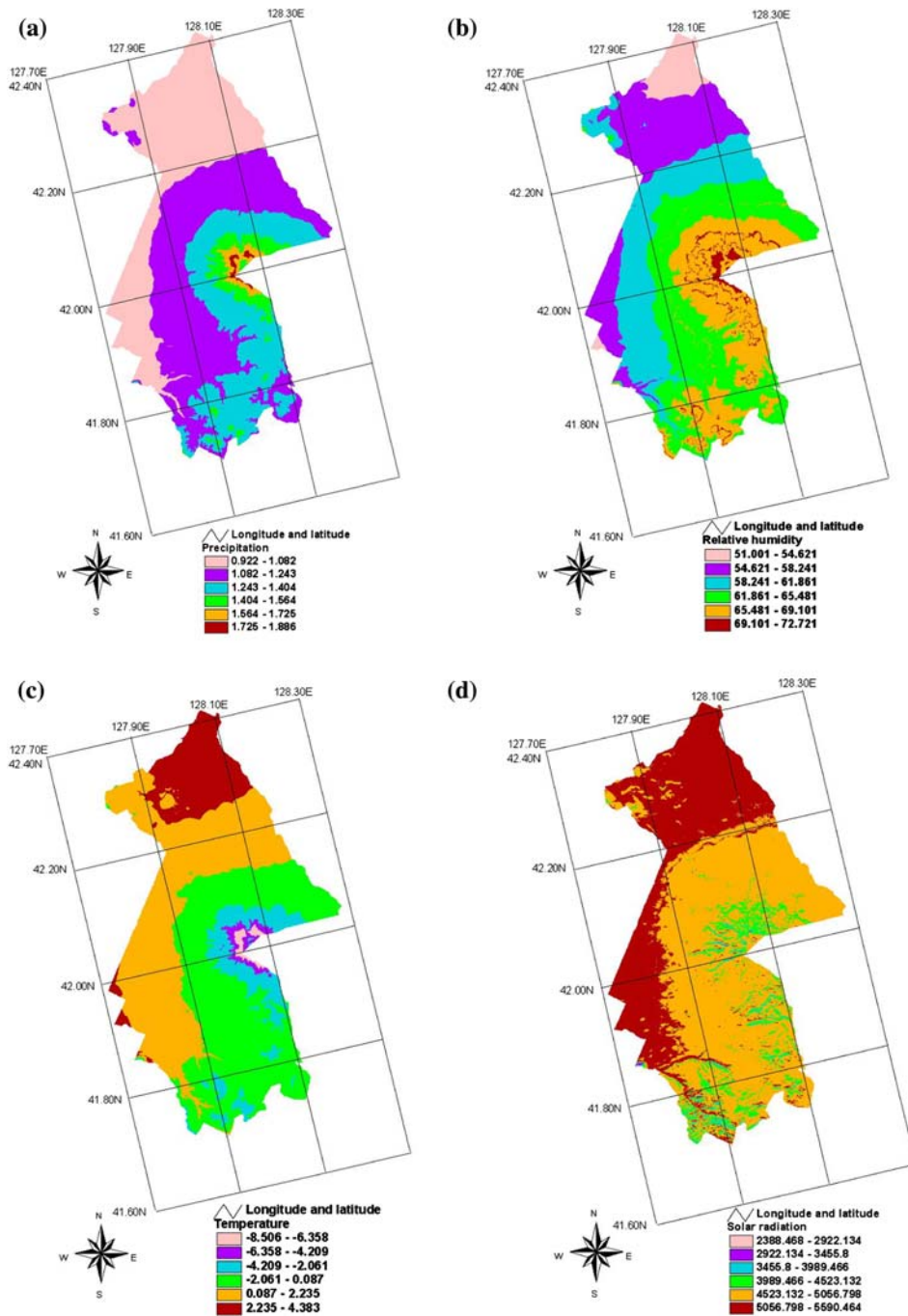


Fig. 2 Spatial pattern of meteorological conditions in the Changbai Mountain Nature Reserve in 1995: **(a)** annual total precipitation (mm yr^{-1}), **(b)** annual mean

relative humidity (%), **(c)** annual mean air temperature ($^{\circ}\text{C}$), and **(d)** annual total solar radiation ($\text{MJ m}^{-2} \text{yr}^{-1}$)

groundwater was not considered. Most of these processes are modeled the same way as in BEPS (Liu et al. 1997, 1999), but the leaf

boundary aerodynamic resistance (r_a), an important parameter for transpiration, is computed as follows:

Table 1 Vegetation types in the Changbai Mountain Nature Reserve

Vegetation type	Relative area (%)	Modeled mean NPP (kgC m ⁻² yr ⁻¹)	Relative error of modeled NPP ^a
Spruce-fir forests	35.15	0.626 ± 0.337	- 0.00635
Mixed broad-leaved and Korean pine forests	25.67	1.084 ± 0.342	0.0730
Poplar and birch forests	15.25	0.466 ± 0.110	- 0.342
Changbai larch forests	7.91	0.753 ± 0.344	0.491
Shrubs	6.40	0.295 ± 0.046	-
Meadows	4.29	0.595 ± 0.136	0.308
Alpine tundra	2.90	0.259 ± 0.067	1.421
<i>Betula ermanii</i> forests	2.21	0.177 ± 0.077	- 0.311
Alpine barren lands	0.22	0.0872 ± 0.0512	5.459
Total	(100%)	0.680 ± 0.395	-

^a Relative error = (modeled NPP - measured NPP)/measured NPP

$$ra = \frac{rh \times rr}{rh + rr} \tag{5}$$

where *rh* is the aerodynamic resistance to convective heat transfer (s m⁻¹), and *rr* is the aerodynamic resistance to radiative heat transfer through air (s m⁻¹). *rr* is calculated as:

$$rr = \frac{\rho \times CP}{4.0 \times SBC \times tk^3} \tag{6}$$

where *rho* is the air density (kg m⁻³), *CP* is the specific heat of air (J kg⁻¹ K⁻¹), *SBC* is the Stefan-Boltzmann constant (5.67e⁻⁸ W m⁻² K⁻⁴), and *tk* is the air temperature (K).

The carbon cycle submodel simulates light utilization, photosynthesis (GPP), autotrophic respiration, carbon allocation in plants, NPP, heterotrophic respiration (*R_h*), and net ecosystem productivity (NEP). Light utilization is computed as the ratio of net carbon absorption to absorbed photosynthetically active radiation (APAR), while all other processes are modeled as in BEPS (Liu et al. 1999). NPP is computed as follows:

$$\begin{aligned} NPP &= GPP - R_a \\ &= GPP - (R_{m,b} + R_{m,s} + R_{m,r} + R_{m,night}) \\ &\quad - (R_{g,b} + R_{g,s} + R_{g,r} + R_{g,night}) \end{aligned} \tag{7}$$

where *R_a* is the autotrophic respiration, *R_{m,b}*, *R_{m,s}*, *R_{m,r}*, and *R_{m,night}* are the maintenance respiration for branches, stems, roots, and nighttime leaves, and *R_{g,b}*, *R_{g,s}*, *R_{g,r}*, and *R_{g,night}* are the growth respiration for these plant components.

NEP is the net exchange of carbon between an ecosystem (including vegetation and soil) and the atmosphere, and is computed as the difference between NPP and *R_h*. Annual change in NPP is determined by net change in live biomass (*ΔB*), litterfall (*L_B*), biomass loss due to grazing (*G_B*), and biomass loss due to human harvesting (*H_B*), i.e.:

$$NPP = \Delta B + L_B + G_B + H_B. \tag{8}$$

Based on empirical observations in CMNR, our study assumed *H_B* to be zero and *G_B* to be 2% of NPP. Also, previous research in this area (Chen et al. 1984) has shown that *L_B* decreases with elevation (*h*) linearly:

$$L_B = 0.237 - 0.0000840h \ (R^2 = 0.852). \tag{9}$$

Inputs to FLPM include (1) initial values for site conditions (geographic coordinates, elevation, slope, aspect, vegetation type, soil type, snow pack, and soil water content), (2) data for driving variables (daily maximum, minimum and mean temperatures, precipitation, total solar radiation, humidity, wind speed, and air pressure), and (3) data for other auxiliary variables including daily LAI and leaf, branch, stem and root biomass. Main outputs of FLPM include NPP, GPP, NEP, autotrophic respiration, soil heterotrophic respiration, evapotranspiration, light utilization efficiency, water utilization efficiency, surface runoff, and soil water content. For this study, we were most interested in NPP and NEP for different ecosystems within CMNR.

Data processing and model parameterization

Maps of vegetation and soil types were compiled from data provided by Institute of Applied Ecology of the Chinese Academy of Sciences. The vegetation map was used for estimating LAI and biological parameters. Slope and aspect maps were produced from an elevation map, which was then used for interpolating meteorological data at different elevations. Soil field water capacity (SFWC) was estimated according to its empirical relationship to elevation (E) previously established for the study area (Yan and Zhao 1995): $SFWC = 325 - 0.05E$. Soil wilting coefficient (SWCF) was estimated on the basis of the assumption that the ratios of SFWC to SWCF for different soil types were approximately constant, and soil dry bulk was defined based on soil types and field observations (e.g., Pei et al. 1981; Xing 1988). We used cloud-free Landsat thematic mapper (TM) imagery to produce the annual maximum normalized difference vegetation index (NDVI) which in turn was used to derive input data including LAI and leaf biomass.

Filed measurements were made during the growing seasons in 99 plots, each about 600 m², within different forest ecosystem types near CMNR by the State Forestry Administration, China (1989–1993). Field-based and remote sensing data were used in combination to compute the spatiotemporal distribution of LAI and biomass at the landscape scale. This was done by applying species-specific the allometric relationships among LAI, biomass, and diameter at breast height (DBH) (Chen and Zhu 1989; Yan and Zhao 1995) and the NDVI–LAI relationships that were developed during this study (Table 2). The growing season was divided into three periods, and leaf biomass and LAI were

estimated accordingly based on the phenology of each vegetation type (see Zhang et al. 2003a for details).

Meteorological data used by FLPM include precipitation, mean, maximum and minimum air temperature, wind speed, air pressure, soil temperature, daylight and night mean air temperature, vapor pressure (deficit), relative humidity, day length, total solar radiation, direct solar radiation, and solar zenith angle. These data were gridded, and values for each grid cell (30 by 30 m to match TM data) were interpolated by using empirical and theoretical relationships (Zhang et al. 2003b, d). The grid cell-level meteorological results were then compared with direct measurements at a number of sites within CMNR, and the degree of agreement was high (Zhang et al. 2003d).

Patch-level model validation and upscaling scheme

Validation of FLPM at the local ecosystem level

Because of the lack of direct measurements of ecosystem productivity at the CMNR landscape scale, which was indeed the primary motivation for this study in the first place, we validated FLPM at 12 sites representing different ecosystem types across the study area. The modeled annual mean NPP agreed with field measurements reasonably well ($R^2 = 0.74$, $n = 12$; Fig. 3). The model did particularly well for the two most dominant forest types that covered nearly 61% of CMNR in area: the relative error was 7.3% for mixed broad-leaved and Korean pine forests and 0.6% for spruce-fir forests (Table 1).

Table 2 Relationships between NDVI and LAI and between LAI and biomass (kg m⁻²) for forests in the Changbai Mountain Natural Reserve

Relationship	R^2	P	N
$LAI = -19.002 - 32.328 \ln(1-NDVI)$	0.496	0.000	99
$LB = -0.664 + 0.921 \ln(LAI)$	0.532	0.000	99
$BB = 0.266 LAI^{0.937}$	0.602	0.000	99
$SB = 2.127 LAI^{0.934}$	0.471	0.000	99
$RB = 0.582 LAI^{0.806}$	0.541	0.000	99

LB = leaf biomass, BB = branch biomass, SB = stem biomass, and RB = root biomass

Scheme for upscaling to the landscape

In order to achieve our research goal, the local-scale ecosystem model must be scaled up to the entire CMNR landscape. To do this, we followed the hierarchical patch dynamic scaling strategy, assuming that the functionality of the landscape is the totality of all its component patches (Wu and Loucks 1995; Wu 1999). A patch was defined as a local ecosystem with similar plant species, age class, and richness, which consisted of multiple grid cells of 30 by 30 m in size. This particular spatial resolution (30 by 30 m) was dictated by the use of TM data, and also considered appropriate for capturing the spatial variations of most biophysical parameters of interest in CMNR. The local ecosystem model was run for all patches with spatially varying input parameter and variable values, and the landscape-level variables of interest were then computed through summation of the patch-level outputs.

In spatial extrapolation through modeling, we explicitly considered the interactions of each patch with the atmosphere and soil, but horizontal interactions between patches were not explicitly considered. This is essentially the “direct extrapolation” method that has been widely used in landscape ecology, particularly for simulating ecosystem productivity (King 1991; Law et al. 2006; Wu and Li 2006). The vegetation and soil characteristics of CMNR exhibited relatively discrete patches (Ge et al. 1990), which made the hierarchical patch dynamic approach quite appropriate.

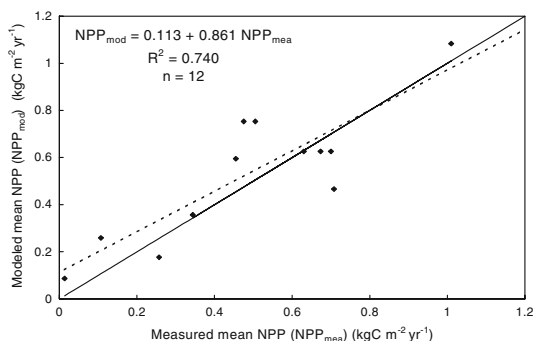


Fig. 3 Comparison of measured and modeled annual mean NPP for 12 observation sites of different vegetation types in the Changbai Mountain Nature Reserve in 1995

Simulation results

Seasonal variations in productivity

With a temporal grain size of a day, FLPM was ideal for examining fine-scale dynamics of NPP in time. We were interested in understanding how NPP changed seasonally for the CMNR landscape in 1995. Our simulations showed conspicuous seasonal changes in NPP of different ecosystem types as well as in mean LAI, stomatal conductance, canopy conductance, maintenance respiration, and growth respiration (Fig. 4). The model predicted that the average NPP was $0.125 \text{ kg C m}^{-2}$ in spring (Mar–May), $0.465 \text{ kg C m}^{-2}$ in summer (June–Aug), $0.0859 \text{ kg C m}^{-2}$ in fall (Sept–Nov), and $0.00484 \text{ kg C m}^{-2}$ in winter (Dec–Feb) for the entire landscape. The NPP in winter was about two orders of magnitude lower than that in summer. This suggests that NPP from spring to autumn would be an adequate estimate of annual NPP. All vegetation types reached their peak productivity in July, with an average NPP of $0.00613 \text{ kg C m}^{-2} \text{ d}^{-1}$ and an average NEP of $0.00518 \text{ kg C m}^{-2} \text{ d}^{-1}$. NPP for mixed broad-leaved and Korean pine forests, spruce-fir forests, and Changbai larch forests were positive year-round, whereas NPP of other vegetation types was slightly negative in the first 4 or 5 months and the last 3 or 4 months of the year (Fig. 4).

In general, the seasonal variations of GPP, respiration, NEP, and transpiration showed a similar pattern to that of NPP because they were affected by the same set of environmental and biological variables, including temperature, precipitation, total solar radiation, relative moisture, wind speed, soil water content, LAI, stomatal conductance, and canopy conductance. These seasonal variations seemed to be influenced most strongly by changes in precipitation and LAI. Across all vegetation types, the seasonal variations of NPP and transpiration were significantly correlated ($r = 0.991$).

Spatial pattern of annual productivity

The annual NPP for the CMNR landscape in 1995 modeled by FLPM was quite heterogeneous in space (Fig. 5a). The annual NPP for the

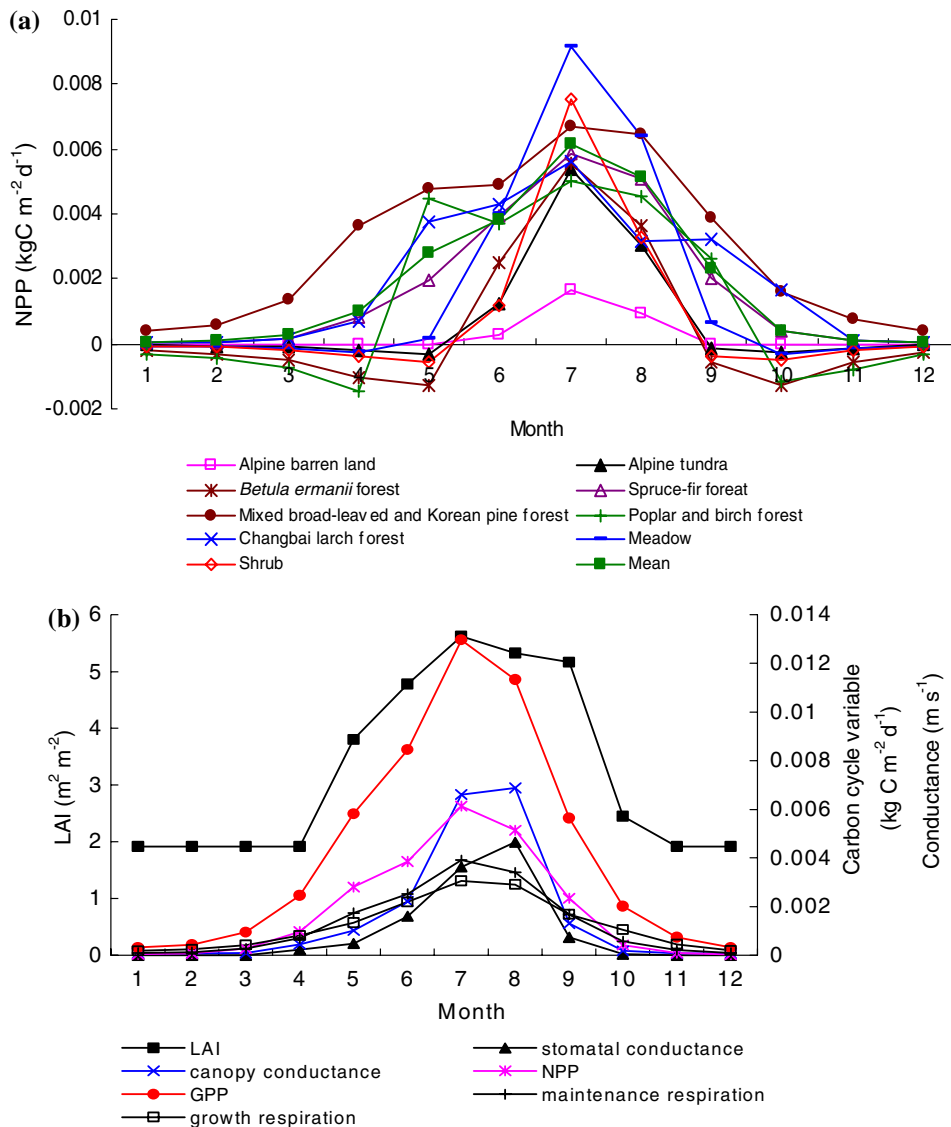


Fig. 4 Seasonal variations of modeled NPP for different vegetation types (a), and seasonal variations of mean LAI, stomatal conductance, canopy conductance, NPP, GPP, maintenance respiration, and growth respiration (b)

entire reserve was $0.680 \pm 0.395 \text{ kg C m}^{-2} \text{ yr}^{-1}$ (Table 1). Among all vegetation types, the mixed broad-leaved and Korean pine forest had the highest annual mean NPP ($1.084 \pm 0.342 \text{ kg C m}^{-2} \text{ yr}^{-1}$). The maximum NPP of this mixed forest was $1.355 \text{ kg C m}^{-2} \text{ yr}^{-1}$, close to the potential productivity of $1.399 \text{ kg C m}^{-2} \text{ yr}^{-1}$ reported by Jin et al. (1995). Spruce-fir forests and Changbai larch forests had the next highest NPP, whereas *Betula ermanii* forests had the lowest NPP among forest types (Table 1). Alpine barren lands had the lowest NPP ($0.0872 \pm$

$0.0512 \text{ kg C m}^{-2} \text{ yr}^{-1}$) of all vegetation types (Table 1). The annual NPP for spruce-fir forests varied with aspect, with lower NPP (-0.10 – $0.060 \text{ kg C m}^{-2} \text{ yr}^{-1}$) on northwestern-facing slopes (270 – 360°), probably because of prevalent wind in that direction.

By summing up NPP for all vegetation types, the total NPP of CMNR was estimated to be $1.323 \text{ Mt C yr}^{-1}$ in 1995. The mixed broad-leaved and Korean pine forest and the spruce-fir forest were the most productive ecosystems in this region, accounting for 73.28% of the total NPP of

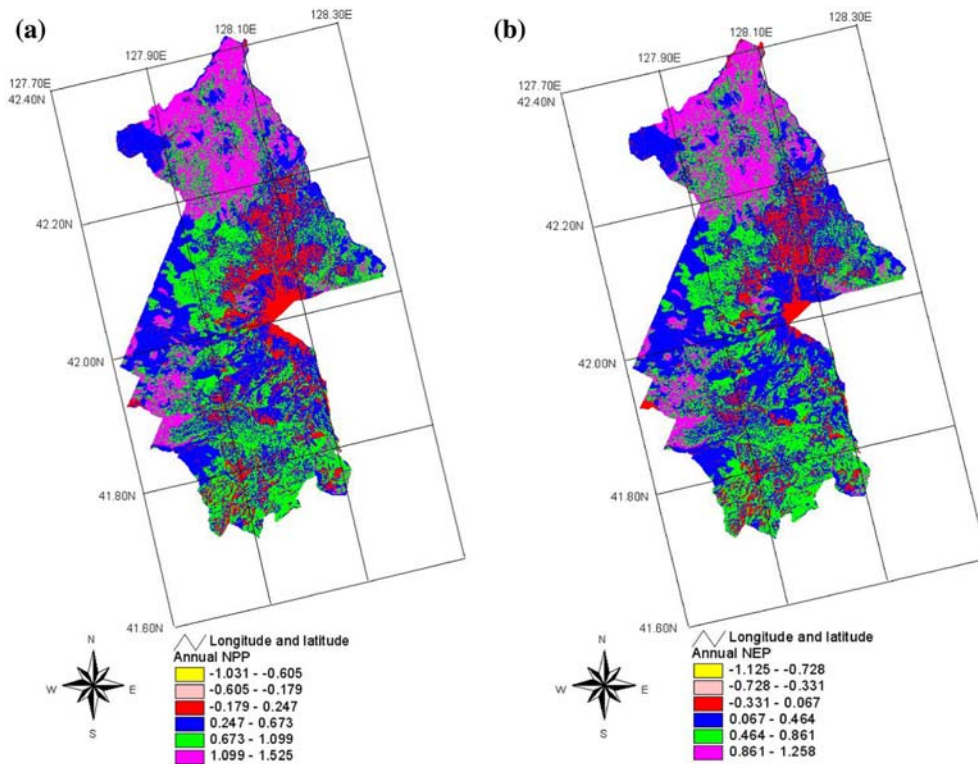


Fig. 5 Spatial pattern of modeled annual NPP (a) and annual NEP (b) of the Changbai Mountain Nature Reserve in 1995 ($\text{kg C m}^{-2} \text{yr}^{-1}$)

the landscape (Table 1). Poplar and birch forests and Changbai larch forests contributed about 10% to the total NPP, respectively.

Relationship of NPP to environmental variables

A number of meteorological variables were correlated with NPP, including (in the order of decreasing Pearson correlation r): relative humidity, air temperature, precipitation, wind speed, and total solar radiation. With increasing elevation, precipitation, relative humidity and wind speed increased, and air temperature and solar radiation decreased. These environmental gradients significantly affected the spatial pattern of NPP in CMNR (compare Figs. 2 and 5a). Higher total solar radiation or air temperature generally resulted in higher NPP, whereas higher wind speed, precipitation, and relative humidity were correlated with lower NPP. Therefore,

meteorological conditions were generally more favorable for plant growth at lower than higher elevations. Soil water content was highly negatively correlated with NPP ($r = -0.650$). However, different vegetation types did not respond to changes in environmental conditions in the same way. For example, the NPP of *Betula ermanii* forests and poplar and birch forests showed quite different responses to temperature and temperature-related meteorological variables than other vegetation types because the autotrophic respiration of these forests was more sensitive to temperature changes (Zhang et al. 2003c).

Carbon source-sink relationship

NEP was computed as the difference between NPP and soil heterotrophic respiration in FLPM. When $\text{NEP} > 0$, the ecosystem is considered a carbon sink (i.e., it absorbs more carbon than it

releases); when $NEP < 0$, the ecosystem is a carbon source (i.e., it releases more carbon than it absorbs). Because of spatial heterogeneity, whether an ecosystem is a source or a sink is bound to be affected by the scale of analysis. Our results showed that the NEP of CMNR was $0.467 \pm 0.346 \text{ kg C m}^{-2} \text{ yr}^{-1}$ without considering harvesting and grazing, and it was reduced to $0.454 \pm 0.338 \text{ kg C m}^{-2} \text{ yr}^{-1}$ when grazing was considered. This means that the CMNR landscape as a whole was a carbon sink, sequestering 0.884–0.909 Mt C for the year of 1995.

However, different types of ecosystems varied greatly in terms of the strength of carbon sink (Fig. 5b). Mixed broad-leaved and Korean pine forests functioned as the strongest carbon sink, with an NEP of $0.777 \pm 0.316 \text{ kg C m}^{-2} \text{ yr}^{-1}$, and spruce-fir forests, Changbai larch forests, and meadows also showed relatively strong carbon sinks (NEP at 0.40–0.50 $\text{kg C m}^{-2} \text{ yr}^{-1}$). The two dominant forest types, the mixed broad-leaved and Korean pine forest and the spruce-fir forest, together accounted for 74.7% of the total NEP of CMNR. Poplar and birch forests, shrubs, and alpine tundra had low values of NEP (about $0.20 \text{ kg C m}^{-2} \text{ yr}^{-1}$), whereas *Betula ermanii* forests and alpine barren lands showed little capacity for sequestering carbon. Increase in live biomass was the primary determinant for the strength of carbon sinks. The decomposition rate of soil organic matter for the entire reserve was $0.167 \text{ Mt C yr}^{-1}$, which was higher than the annual rate of litterfall. But the spatial variation in the decomposition rate among different vegetation types was also high. For example, the decomposition rate was 0.5–1.0 times higher than the litterfall rate for forest types, while these two rates were about the same for alpine tundra and alpine barren lands.

Discussion

Extrapolating ecosystem processes from local patches to the landscape and regional scales is a central issue in ecology, but remains a grand challenge today (Wu et al. 2006). To quantify the spatial pattern of ecosystem processes in the Changbai Mountain Nature Reserve in China,

this study provides an example of upscaling eco-physiological and geophysical processes from the patch level to the entire landscape by integrating simulation modeling, GIS, remote sensing, and field-based observations. While the general scaling approach is similar to those used in other studies (e.g., King 1991; Wu 1999; Law et al. 2006), this research has resulted in new findings that are particularly useful for understanding the structure and functioning of the CMNR landscape as well as unraveling problems and challenges in scaling up ecosystem processes across heterogeneous landscapes.

Our modeling results showed that meteorological conditions are critically important determinants of the primary productivity of ecosystems through direct and indirect effects on carbon and water cycling processes. However, the landscape-level pattern of ecosystem processes is ultimately determined by the interactions between biological communities and environmental factors. The mixed broad-leaved and Korean pine forest is the most extensive and productive ecosystem type in the Changbai Mountain region while a diversity of other ecosystem types also exist. Our study indicated that the Changbai Mountain Reserve as a whole functioned as a carbon sink for the year of 1995. Because the carbon source-sink relation for a landscape composed of different ecosystem may change in both space and time, a longer period of time (e.g., decades) is needed to confirm this finding. Based on this and other studies in the CMNR area, however, we speculate that this general conclusion should hold for most years although the relative strength of the carbon sink may change in response to fluctuations in environmental conditions and disturbances. Our study indicated that mixed broad-leave and Korean pine forests and spruce-fir forests played the most important role in carbon sequestration in this area because of their high NEP and extensive distribution. As these ecosystems are widely found in northeastern China, these findings are of regional importance (Jin et al. 2000).

Our model predictions of NPP agreed quite well with field observation for the major ecosystem types in this region, but improvements are clearly needed for some of the ecosystem types that occupy in small areas. In particular, the

model underestimated the NPP of *Betula ermanii* forests and poplar and birch forests by more than 30% whereas significantly overestimating the NPP of meadow, Changbai larch forests, alpine tundra, and alpine barren lands. Causes for these large discrepancies may include: (1) errors in estimating LAI and biomass from remote sensing data for these systems of small areas, and consequently inaccuracy in the NDVI–LAI and LAI–biomass relationships, (2) errors in ground-based measurements, and (3) differences in spatial and temporal scales of modeled versus measured data. More extensive field observations as well as model refinements are needed to address these problems in the future.

Sun et al. (2004) used the original BEPS model to simulate NPP and evapotranspiration of the north slope of CMNR for the year of 2001. Their study site included part of the reserve and some urban and agricultural lands outside the reserve. Their land cover classes included broad-leaved forest, coniferous forest, mixed forest, cropland, alpine tundra and shrub, urban, and water. For those categories shared by FLPM and BEPS, the NPP predictions from the two models were comparable but different, with a relative difference ranging from 2.5% to 53.8%. These discrepancies may be attributable to a number of factors, including differences in meteorological conditions between 1995 and 2001, methods for estimating daily meteorological data, LAI and biomass, and formulations of some processes in the two models. Our future work will include an in-depth examination of these possible causes.

Our future work will also include a systematic uncertainty analysis with input data and model parameters following methods recommended by Li and Wu (2006). In particular, the accuracy of estimated LAI strongly affects the accuracy of some key carbon and water cycling variables, including canopy radiation absorption, canopy stomatal conductance, photosynthesis, maintenance respiration, transpiration, canopy rainfall interception, and soil evaporation. Therefore, reliable estimates of LAI are an important prerequisite for the successful application of FLPM at landscape and regional scales. The empirical NDVI–LAI relationship derived from remote sensing data seemed to work reasonably well in

this study, but further test and refinement are needed with daily MODIS LAI data and LAI measurements made with tracing instruments. Accuracy in vegetation classification directly affects a suite of physiological and ecosystem parameters, and we expect that more advanced remote sensing techniques will help reduce the degree of arbitrariness in vegetation mapping in the future. In addition, nitrogen cycling, ground-water runoff, and disturbance regime will be considered in future versions of FLPM.

Through a perpetuating cycle of modification and evaluation, we will continue to improve the model performance, use it to explore ecosystem responses of CMNR to climate and land use change, and test different scaling approaches. The results of these on-going and future studies will also provide critically needed information for management purposes in this region.

Acknowledgements We are grateful to Renchang Bu for providing digital maps of vegetation, soil, and elevation, Zengxiang Zhang and Mingliang Liu for Landsat TM images, and the Changbai Mountain Forest Ecosystem Research Station of the Chinese Academy of Sciences for meteorological data. Jone Liu and Jinming Chen graciously helped with the code of BEPS. We thank three anonymous reviewers for their helpful comments on the manuscript, and Xiaodong Yan, Xuyong Li, Bin Shao, and Baowen Chen for helpful discussions on the study design. This research was supported by National Natural Science Foundation of China (NSFC) (30500076), Natural Science Fund for Distinguished Young Scholars (30225012), NSFC (39970613), and Knowledge Innovation Programs of the Chinese Academy of Sciences (KZCX3-SW-218).

References

- Aber JD, Burke IC, Acock B, Bugmann HKM, Kabat P, Menaut J-C, Noble IR, Reynolds JF, Steffen WL, Wu J (1999) Hydrological and biogeochemical processes in complex landscapes. In: Tenhunen JD, Kabat P (eds) Integrating hydrology, ecosystem dynamics, and biogeochemistry in complex landscapes. Wiley, Chichester, pp 335–355
- Band L, Peterson D, Running S (1991) Forest ecosystem processes at the watershed scale: basis for distributed simulation. *Ecol Model* 56:171–196
- Burke I, Schimel D, Yonker CM, Parton WJ, Joyce LA, Lauenroth WK (1990). Regional modeling of grassland biogeochemistry using GIS. *Landscape Ecol* 4:45–54
- Chen BR, Xu GS, Ding GF, Zhang YH, Wang W (1984) Litterfall and nutrient contents of major forest ecosystems in Changbai Mountain. In: Changbai Moun-

- tain Forest Ecosystem Research Station (ed) Forest Ecosystem Study (IV). Chinese Forestry Press, Beijing, China, pp 19–22
- Chen CG, Zhu JF (1989) Manual on biomass of main trees in northeastern China. Chinese Forestry Press, Beijing, China
- Chen JM, Liu J, Cihlar J, Goulden ML (1999) Daily canopy photosynthesis model through temporal and spatial scaling for remote sensing applications. *Ecol Model* 124:99–119
- Coughlan JC, Running SW (1997) Regional ecosystem simulation: a general model for simulating snow accumulation and melt in mountainous terrain. *Landscape Ecol* 12:119–136
- Dai Y, Dickinson RE, Wang YP (2004) A two-big-leaf model for canopy temperature, photosynthesis, and stomatal conductance. *Am Meteorol Soc* 6:2281–2299
- Ge JP, Guo HY, Chen D (1990) Study on population structure of natural Korean pine forests in Xiao Xing'anling. *J Northeast For Univ* 18:26–32
- Hong B, Swaney DP, Weinstein DA (2006) Simulating spatial nitrogen dynamics in a forested reference watershed, Hubbard Brook Watershed 6, New Hampshire, USA. *Landscape Ecol* 21:195–211
- Jin CJ, Zhu T, Yang SH (1995) Study on the estimation of latent productivity in a broad-leaved Korean pine forest of Changbai Mountain. *Acta Ecol Sin* 15(Supp. B):86–92
- Jin CJ, Guan DX, Zhu TY (2000) Spectral characteristics of solar radiation in broad-leaved Korean pine forest in Changbai Mountain. *Chin J Appl Ecol* 11:19–21
- Kennedy RE, Turner DP, Cohen WB, Guzy M (2006) A method to efficiently apply a biogeochemical model to a landscape. *Landscape Ecol* 21:213–224
- King AW (1991) Translating models across scales in the landscape. In: Turner MG, Gardner RH (eds) Quantitative methods in landscape ecology. Springer-Verlag, New York, pp 479–517
- Law BE, Turner D, Campbell J, Lefsky M, Guzy M, Sun O, Tuyl SV (2006) Carbon fluxes across regions: observational constraints at multiple scales. In: Wu J, Jones KB, Li H, Loucks OL (eds) Scaling and uncertainty analysis in ecology: methods and applications. Springer, Dordrecht, The Netherlands, pp 167–190
- Li H, Wu J (2006) Uncertainty analysis in ecological studies: an overview. In: Wu J, Jones KB, Li H, Loucks OL (eds) Scaling and uncertainty analysis in ecology: methods and applications. Springer, Dordrecht, The Netherlands, pp 45–66
- Liu J, Chen JM, Cihlar J, Park WM (1997) A process-based boreal ecosystem productivity simulator using remote sensing inputs. *Remote Sens. Environ* 62:158–175
- Liu J, Chen JM, Cihlar J, Chen W (1999) Net primary productivity distribution in the BOREAS region from a process model using satellite and surface data. *J Geophys Res* 104:27735–27754
- Mladenoff DJ, Baker WL (1999) Spatial modeling of forest landscape change: approaches and applications. Cambridge University Press, New York
- Norman JM (1982) Simulation of microclimates. In: Hatfield JL, Thomason IJ (eds) Biometeorology in integrated pest management. Academic Press, New York, pp 65–99
- Parton WJ, Schimel DS, Cole CV, Ojima DS (1987) Analysis of factors controlling soil organic matter levels in Great Plains grasslands. *Soil Sci Soc Am J* 51:1173–1179
- Pei TP, Sun JZ, Lu FY, Chi ZW (1981) Mathematic model for infiltration coefficient of forest soil. In: Changbai Mountain Forest Ecosystem Research Station (ed) Forest Ecosystem Study (II). Chinese Forestry Press, Beijing, China, pp 189
- Running SW, Coughlan JC (1988) A general model of forest ecosystem processes for regional applications. I. Hydrologic balance, canopy gas exchange and primary production processes. *Ecol Model* 42:125–154
- Running SW, Hunt ER (1993) Generalization of a forest ecosystem process model for other biomes, BIOME-BGC, and an application for global-scale models. In: Ehleringer JR, Field CB (eds) Scaling ecological processes: leaf to globe. Academic Press, San Diego, pp 141–158
- Sun R, Chen JM, Zhu QJ, Zhou YY, Liu J, Li JT, Liu SH, Yan GJ, Tang SH (2004) Spatial distribution of net primary productivity and evapotranspiration in Changbaishan Natural Reserve, China, using Landsat ETM+ data. *Can J Remote Sens* 30:731–742
- Turner MG, Gardner RH, O'Neill RV (2001) Landscape ecology in theory and practice: pattern and process. Springer-Verlag, New York
- Turner MG, Cardille JA (2006) Spatial heterogeneity and ecosystem processes. In: Wu J, Hobbs R (eds) Key Topics in Landscape Ecology. Cambridge University Press, Cambridge, UK (in press)
- Waring RH, Running SW (1998) Forest ecosystems: analysis at multiple scales. Academic Press, San Diego
- Wu J, Levin SA (1994) A spatial patch dynamic modeling approach to pattern and process in an annual grassland. *Ecol Monogr* 64:447–464
- Wu J, Loucks OL (1995) From balance-of-nature to hierarchical patch dynamics: a paradigm shift in ecology. *Q Rev Biol* 70:439–466
- Wu J, Levin SA (1997) A patch-based spatial modeling approach: conceptual framework and simulation scheme. *Ecol Model* 101:325–346
- Wu J (1999). Hierarchy and scaling: extrapolating information along a scaling ladder. *Can J Remote Sens* 25:367–380
- Wu J, Hobbs R (2002) Key issues and research priorities in landscape ecology: an idiosyncratic synthesis. *Landscape Ecol* 17:355–365
- Wu J, Jones KB, Li H, Loucks OL (2006) Scaling and uncertainty analysis in ecology: methods and applications. Springer, Dordrecht, The Netherlands
- Wu J, Li H (2006) Perspectives and methods of scaling. In: Wu J, Jones KB, Li H, Loucks OL (eds) Scaling and uncertainty analysis in ecology: methods and applications. Springer, Dordrecht, The Netherlands, pp 17–44

- Xing SP (1988) Forests of jilin province. Jilin Science and Technology Press, Changchun, Chinese Forestry Press, Beijing, China
- Yan XD, Zhao SD (1995) CHANGFOR a computer model for forest growth and succession in Changbai Mountain. *Acta Ecol Sin* 15(Supp. B):86–92
- Zhang N, Yu GR, Yu ZL, Zhao SD (2003a) Simulating leaf area index and biomass at the landscape scale. *J Geogr Sci* 13:139–152
- Zhang N, Yu GR, Yu ZL, Zhao SD (2003b) Simulation of temporal and spatial distribution of natural vegetation light utilization efficiency based on 3S. *Acta Phytoecol Sin* 27:325–336
- Zhang N, Yu GR, Yu ZL, Zhao SD (2003c) Analysis of factors affecting the spatial distribution of net primary productivity in the Changbai Mountain using a process model. *Chin J Appl Ecol* 14:659–664
- Zhang N, Yu GR, Zhao SD, Yu ZL (2003d) Landscape-scale ecosystem productivity modeling using remote sensing and land surface data. *Chin J Appl Ecol* 14:643–652